Journal of the Association of Arab Universities for Basic and Applied Sciences (2013) **14**, 1–8

University of Bahrain

Journal of the Association of Arab Universities for Basic and Applied Sciences

www.elsevier.com/locate/jaaubas
www.sciencedirect.com

تقدير بخار الماء الراسب باستخدام ضغط البخار و درجة الحرارة في منطقة جافة في وسط المملكة العربية السعودية

عبدالرحمن مغربي، حاتم الدعجاني

المركز الوطني للرياضيات والفيزياء، مدينة الملك عبدالعزيز للعلوم والتقنية، المملكة العربية السعودية

الملخص:

يعتبر بخار الماء الراسب من أهم مكونات الغلاف الجوي وله تأثير ملحوظ على الكثير من العمليات الجويه. هذا العامل الفيزيائي يصعب قياسه بدقة عالية فى نفس الزمان أو المكان في جميع الظروف الجوية. في هذا البحث، تم استخدام بيانات الراديوسوند لمدينة الرياض في وسط المملكة العربية السعودية للفترة الزمنية ما بين 1985 إلى 2007م لنمذجة بخار الماء الراسب وذلك من خلال قياس ضغط البخار ودرجة حرارة الهواء. هذا النموذج المتعدد المتغيرات، يعتبر إحصائيا غير منحاز وله معامل ارتباط يساوي 0.81 ومتوسط انحياز الخطاء يساوي -0.06mm والانحراف المعياري 2.80mm. بعد ذلك تم اختبار أداء النموذج الرياضي المقترح باستخدام مجموعتين غير معتمدتين من البيانات: المجموعة الأولى من البيانات هي لأربع سنوات ونصف من قياسات الراديوسوند للبخار الراسب للفترة الزمنية 2008 إلى مارس 2012م، بينما المجموعة الثانية من البيانات هي عبارة عن بيانات بخار الماء الراسب لسنتين والتي تم الحصول عليها من بيانات الطيف الشمسي عند الطول الموجي 940nm. لكلا المجموعتين كان توقع النموذج الرياضي ممتاز حيث كان متوسط إنحياز الخطأ أقل من 1mm وكان الانحراف المعياري للمجموعة الأولى 3.12mm و 2.50mm للمجموعة الثانيه. بالإضافة إلى ذلك فقد تم في هذا البحث إختبار قدرة آداء 15 نموذج رياضي منشوره سابقا على حساب بخار الماء الراسب في الرياض خلال الفترة الزمنية ما بين 1985 إلى 2007. لقد تبين بأن أداء هذه النماذج كان متنوع وأن أداء النموذج المقترح في هذه الدراسه تفوق على أداء جميع هذه النماذج السابقه.

Journal of the Association of Arab Universities for Basic and Applied Sciences (2013) **14**, 1–8

University of Bahrain

Journal of the Association of Arab Universities for Basic and Applied Sciences

www.elsevier.com/locate/jaaubas
www.sciencedirect.com

ORIGINAL ARTICLE

Estimation of precipitable water vapour using vapour pressure and air temperature in an arid region in central Saudi Arabia

Abdullrahman Maghrabi *, H.M. Al Dajani

National Centre For Mathematics and Physics, King Abdulaziz City for Science and Technology, P.O. Box 6086, Riyadh 11442, Saudi Arabia

Received 7 July 2012; revised 4 November 2012; accepted 17 November 2012
Available online 5 January 2013

KEYWORDS

Vapour pressure;
PWV;
Air temperature;
Riyadh;
Radiosonde;
Sun photometer

Abstract Precipitable water vapour (PWV) is an important component of the atmosphere and significantly influences many atmospheric processes. It is a physical parameter that is difficult to measure with adequate spatial and time resolution under all weather conditions. In this study, radiosonde data for the city of Riyadh in central Saudi Arabia (24°43′ N; 46°40′ E, 764 m a.s.l.) from 1985 to 2007 were used to model the precipitable water vapour (PWV) from the measurements of vapour pressure and air temperature. A multilinear model was essentially unbiased with a correlation coefficient (R^2) of 0.81, a mean bias error (MBE) of −0.06 mm, and a root mean square error (RMSE) of approximately 2.80 mm. The performance of the model was tested against two independent datasets. The first dataset was four and half years of radiosonde measurements of PWV for the period 2008–March 2012, and the second set was two years of PWV data obtained from sun photometer measurements at 940 nm. For both datasets, the predictability of the model was excellent, with MBE values of less than 1 mm. The RMSE was 3.21 mm for the first set and 2.50 mm for the second set. The predictive powers of 15 empirical models from the literature were tested against the measured PWV for the period 1985 to 2007. The performances of these models varied. The proposed multilinear model from this study outperforms the overall performance of these 15 models.

1. Introduction

Of the major atmospheric gases, water vapour is the most abundant and has the greatest variability. It possesses many features of interest to scientists.

The water molecule creates strong absorption bands at solar and terrestrial wavelengths. For instance, gaseous absorption and emission of thermal atmospheric radiation are mainly due to water vapour absorption bands below 7.6 μm, between 13 μm and 16 μm, and beyond 22 μm (Lhomme et al., 2007).

* Corresponding author. Tel.: +966 1 481 4302; fax: +966 1 481 3521.
E-mail address: amaghrabi@kacst.edu.sa (A. Maghrabi).
Peer review under responsibility of University of Bahrain.

ELSEVIER Production and hosting by Elsevier

1815-3852
http://dx.doi.org/10.1016/j.jaubas.2012.11.001

Additionally, the vapour phase plays an important role in the hydrological cycle, and it affects the climate and weather systems (e.g. Follette et al., 2008). Its presence attenuates electromagnetic radiation in the atmosphere, which is significant to astronomy, radar, telecommunications and remote sensing. Water vapour, at all levels, strongly affects the temperature of the atmosphere.

Due to the environmental impacts of water vapour, there is increasing interest in its measurement at the surface and in its total abundance in a vertical column through the atmosphere. The latter parameter is called the integrated or precipitable water vapour (PWV), and its measurement is the central subject of this paper. PWV is the amount of liquid water that would be obtained if all the vapour in the atmosphere within the vertical column were compressed to the point of condensation (Dupont et al., 2008).

In contrast to the other greenhouse gases, the amount of PWV in the atmosphere can vary considerably with prevailing conditions, including time of day, wind direction, and temperature. This variability makes PWV an extremely difficult quantity to measure. Additionally, detailed data of the water content are an important input data for hydrological, energetic and radiation models (Smirnov and Moore, 2001; Zhai and Eskridge, 1997; Dai et al., 2002; Cohen et al., 2000; Bokoye et al., 2003).

Although water vapour is important in many different applications, scientists were unable to study its spatial and temporal distribution until radiosonde data became available.

The standard techniques for measuring PWV are radiosondes (Lanzante et al., 2003), ground-based microwave radiometers, LIDAR systems (Gerding et al., 2004; Kuwahara et al., 2008), LASER systems (Eng et al., 1973) and GPS satellites (Bevis et al., 1992; Hagemann et al., 2003; Li et al., 2008; Stoew et al., 2001; Pramualsakdikul et al., 2007). However, each method has limitations. LIDAR measurements are expensive. Low spatial resolution restricts the use of space-based instruments, while radiosondes offer limited coverage (i.e., they can only observe a small number of sites). Another approach involves observing the atmospheric transmittance with sun photometers or equivalent instruments (Torres et al., 2010; Holben et al., 2001; Elies et al., 2010). Algorithms and techniques to derive the PWV from temperature measurements by infrared (IR) radiometers have been explored (Maghrabi et al., 2009; Maghrabi and Clay, 2010; Clay et al., 1998; Brooks et al., 2007).

When the required PWV data are scarce, the use of empirical models is a common practice (Maghrabi, 2009; Iqbal, 1983; Hussain, 1984; Guerova et al., 2005). The empirical methods are based on the statistical fit between the PWV data and screen-level parameters, such as specific humidity, dew point temperature, air temperature, and relative humidity. Several parametric models of PWV have been developed based on empirical data (e.g. Gueymard, 1994; Butler, 1998a,b; Hsu and Blanchard, 1989; Tuller, 1977; Adeyemi 2009a,b; Viswanadham, 1980; Adedokun 1986).

For instance, Reitan (1963) found a linear relationship between the monthly mean surface dew point and the natural logarithm of the PWV. Hussain (1984) developed an empirical model that parameterised PWV as a function of the air temperature and relative humidity. Ruckstuhl et al. (2007) proposed a linear relationship between the GPS-derived PWV and screen-level specific humidity at several sites in Europe.

The main objective of this study is to find a simple model based on screen meteorological variables to parameterise the PWV in arid conditions in the city of Riyadh, which is located in the central Saudi Arabia. This study presents more recent and longer time periods from this part of the world. This region was selected because it is an area of relatively homogeneous observations and one for which the records of changes are available. Moreover, no previous studies have been done to address the PWV estimation in this part of the world.

The details of the experimental site and the methodologies in treating the data and calculating the PWV values are given in Section 2. In Section 3, the results are presented. The conclusions and future research are given in Section 4.

2. Experimental site, data sources and methods

The study area of Riyadh lies in the central region of the Arabian Peninsula (24°43′ N; 46°40′ E, 764 m a.s.l.). The central region is considered to be a vast eroded plateau consisting of areas of uplands, broad valleys and dry rivers. The area also contains a number of marshes, thought to be the remnants of inland seas that existed in ancient geological times. The arid conditions and continentality prevailing at this site are responsible for large seasonal temperature differences, with cool winters and very hot summers. The area experiences extremely low humidity, particularly in the summer (Maghrabi et al., 2011).

The climate of the region exhibits four dominant seasons each year: winter (December–February), spring (March–May), summer (June–August) and autumn (September–November).

Radiosonde and surface data were provided by the Saudi Presidency of Meteorological and Environment (PME). Saudi's atmospheric radiosonde observations date back to the 1970s. Because of the inhomogeneities found in radiosonde data in both temperature and dew point depression prior to 1970, only the data from 1985 to March 2012 were selected. The observations were made using Vaisala RS80A sondes. Pressures, temperatures and dew point depressions were extracted from each sounding at all reported levels (i.e., mandatory and significant levels) from the surface to 300 mb. Data extraction was terminated at 300 mb because of the poor performance of radiosonde humidity sensors at cold temperatures (Elliott and Gaffen; 1991; Wang et al., 2002; Free et al., 2004; Kassomenos and MCGregor, 2006).

Assuming water vapour to be a perfect gas, its absolute humidity ρ at sounding level z was obtained by a classic formula derived from the equation of state of an ideal gas:

$$\rho_v(z) = \frac{217 \times RH(z) \times e(z,T)}{T} \tag{1}$$

where T is the observed absolute temperature, and $RH(z)$ is the relative humidity. The last term is the saturation water vapour pressure $e(z,T)$ in mb, calculated using the standard formula (e.g., Kassomenos and MCGregor, 2006). Integration of Eq. (1) along the vertical profile gives total PWV:

$$PWV = \int_0^z \rho_v(z)dz \tag{2}$$

The methodologies so far assume a complete data series. Unfortunately, this is never the case with real data. Some kind of interpolation is necessary to complete the series. Interpola-

tion must be kept to a reasonable level in order to preserve the nature of the information contained in the data (Zhai and Eskridge, 1996; Dai et al., 2002). In our case, we linearly interpolated up to 5 missing data points. Larger gaps were not considered, and the months that have such large amounts of missing data are excluded from the analysis. After these cuts, a total of 13,150 daily values were available: 6750 of them were from 0000 UT (nighttime) and 6400 were from 1200 UT (daytime). The mean monthly values of the PWV were obtained by taking the average daily values of the PWV for each month during the study period. A total of 325 monthly data points during the 26-year period were obtained. The mean monthly values of the daytime and nighttime levels of PWV were treated separately.

The PWV data measured at 940 nm were obtained from a Cimel automatic sun/sky photometer. This detector was placed at the AERONET site on the rooftop of the solar village (24.91° N, 46.41° E) at an elevation of 764 m and approximately 25 km northwest of Riyadh (Maghrabi et al., 2011). The instrumentation, data acquisition, retrieval algorithms and calibration procedure conform to AERONET standards and are described in detail in numerous studies (Holben et al., 2001). Standard screen-level meteorological observations, such as air temperature, relative humidity, and dew point temperature, were obtained from the Riyadh Airport records and provided by the Presidency of Meteorological Environment (PME).

A summary of the mean maximum and minimum values for some of the meteorological parameters is presented in Table 1.

The work in this paper was conducted with the following three steps.

First, we investigated the relationships between the dependent variable (PWV) and the independent variables (vapour pressure (eo) and air temperature (T)) using radiosonde-derived PWV data from 1985 to 2007. Based on the results of the regression analysis, a multilinear predictive model to predict PWV as a function of the two parameters was proposed. Second, we tested the performance of the proposed model against two independent data sets. The first set (set 1) is a radiosonde-derived PWV covering the period 2008–2012. The second set (set 2) is the PWV obtained from the Cimel sun photometer at 940 nm for the period 2001–2002. In the last step, the PWV predictions by previously reported models were compared to the measured PWV values for the period 1985–2007.

Table 1 The descriptive statistics for the radiosonde-derived PWV (in mm) and the sun photometer PWV at 940 nm. Some meteorological variables (air temperature (T), vapour pressure (eo), and dew point temperature (T_{dew})) for the two considered periods are also shown.

	Mean	Maximum	Minimum
(eo) 1985–2007	7.42	26.12	0.43
(eo) Set 2 PWV at 940 nm	9.22	22.26	2.68
(PWV) 1985–2007	15.24	40.87	2.19
(PWV) Set 2 PWV at 940 nm	12.33	23.92	2.88
(T_{dew}) 1985–2007	0.77	21.50	−27.60
(T_{dew}) Set 2 PWV at 940 nm	5.33	19.23	−10.81
(T) 1985–2007	27.53	47.44	0.20
(T) Set 2 PWV at 940 nm	27.62	38.57	8.09

The performance of the estimated PWV data was assessed based on some commonly used statistical indicators (e.g., Maghrabi, 2009). These include the following: (1) the mean percentage error (MPE), (2) the mean bias error (MBE), and (3) the root mean square error (RMSE). Their functional forms are given as:

$$\mathrm{MPE} = \frac{1}{N}\sum_{i=1}^{N}\left(\frac{\mathrm{PWV}_{imeas} - \mathrm{PWV}_{ical}}{\mathrm{PWV}_{imeas}} \times 100\right), \tag{3}$$

$$\mathrm{MBE} = \frac{1}{N}\sum_{i=1}^{N}(\mathrm{PWV}_{imeas} - \mathrm{PWV}_{ical}), \tag{4}$$

$$\mathrm{RMSE} = \frac{1}{N}\sum_{i=1}^{N}\sqrt{(\mathrm{PWV}_{imeas} - \mathrm{PWV}_{ical})^2}, \tag{5}$$

where PWV_{imeas} is the ith measured value, PWV_{ical} the ith predicted or calculated value, and N is the total number of observations.

The MPE can be defined as the percentage deviation of the predicted and measured PWV data. The MBE reveals whether a given model has a tendency to under- or overpredict, with MBE values close to zero being desirable. The RMSE indicates the level of scatter in a model, providing a term-by-term comparison of the actual deviations between the predicted and observed values. Lower RMSE values reflect a better model in terms of its absolute deviation.

We also used t-statistics (t-stat at a significance level of $\alpha = 0.01$) to determine whether the equation estimates are statistically significant.

3. Results and discussion

3.1. Model parameterisation

In this section, we aim to find an empirical model that correlates the measured PWV data with some screen-level parameters that have a physical link with the PWV. We chose two parameters: vapour pressure and air temperature. Vapour pressure was selected because the water content is concentrated near the surface layer. The air temperature usually affects the

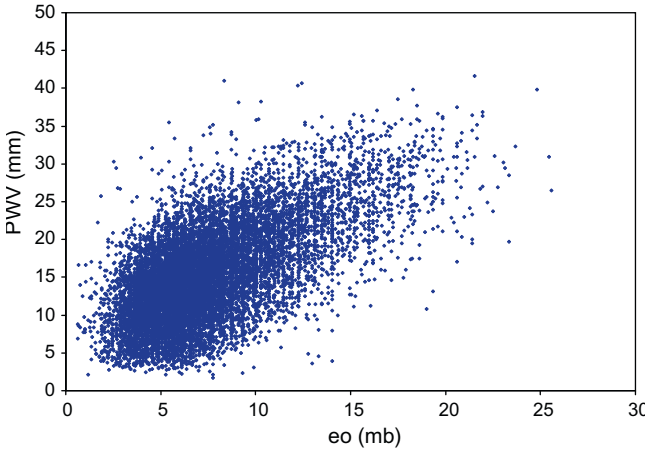

Figure 1 The relationship between daily PWV values and the vapour pressure for all sky conditions.

Table 2 The mean values of the measured and the predicted PWV for the original data (1985–2007), set 1, and set 2. The MBE, RMSE and MPE results for each data set were also given.

	Original set daily 1985–2007	Daily 0000	Daily 1200	Original set monthly 1985–2007	Monthly 0000	Monthly 1200	Yearly	Set 1 2008–2012	Set 2 PWV at 940 nm
Measured PWV (mm)	15.24	15.06	15.49	14.86	14.62	15.12	15.19	15.15	12.74
Predicted PWV (mm)	15.3	14.70	15.07	13.96	12.77	14.58	15.46	15.23	11.63
MBE (mm)	−0.06	0.359	0.42	0.86	1.85	0.54	−0.26	−0.08	0.87
RMSE (mm)	2.80	3.08	3.08	2.83	3.37	3.17	1.00	3.21	2.26
MPE (%)	−7.17	−8.09	8.27	3.31	8.09	−6.34	7.09	−9.37	7.2

atmospheric water content by increasing or decreasing evaporation from the ground as a direct result of the water vapour concentration in the atmospheric layers.

Fig. 1 shows the daily variations of the PWV against the screen-level eo. The PWV was clearly correlated with eo, although there was some spread in the data. The general trend was that PWV increased with eo.

The result of the regression analysis of the relationship between the two parameters is given as:

$$\mathrm{PWV} = 1.15 \times \mathrm{eo} + 6.8, \tag{6}$$

where the correlation coefficients R^2, MBE and RMSE were 0.38, 6.24 mm and 6.41 mm, respectively.

To produce a model that accurately describes the PWV and minimises the errors associated with using a single variable model, multiple regression analysis between the PWV and the two parameters (i.e., eo and T) was performed. The multiple regression analysis yielded the following relationship:

$$\mathrm{PWV} = 2.72 + 1.32 \times \mathrm{eo} + 0.21 \times T \tag{7}$$

Table 2 summarises the mean values of the measured and the predicted PWV for the original data (1985–2007), set 1, and set 2. The MBE, RMSE and MPE results for each data set were also given.

The correlation coefficient R^2 was 0.81, the MBE was −0.06 mm, and the RMSE was 2.80 mm. The use of two variables further optimised the predictions. Fig. 2a shows the estimated PWV based on Eq. (7) plotted against the measured PWV for the period between 1985 and 2007. The model can accurately predict the PWV. The data distributed around the 1:1 line and the maximum deviations of the predicted values are less than two standard deviations from the means of the measured values.

The linear relationship between the measured PWV and the predicted values from Eq. (7) was also statistically tested based on a simple linear regression test at a significance level of $\alpha = 0.05$, where α is one minus the confidence interval. In this test, the confidence interval was 95%. The equation for the regression is

$$\mathrm{PWV\_Predicted} = 0.81 \times \mathrm{PWV\_Measured} + 2.84 \tag{8}$$

with a correlation coefficient of 0.82. This result indicates that the overall regression was statistically significant. The offset of the predicted values from the 1:1 line was approximately 3 mm. Fig. 2b shows that the frequency distribution of the MBE between the measured and predicted values superimposes with the normal distribution curve. The MBE values are confined within ±6 mm. The overall distribution of the errors resembles a normal distribution.

For some situations, the proposed model greatly under- or overestimates the measured PWV values. The large deviations, while consistent with a normal error distribution, can be explained by several factors. For example, the proposed model was considered to be applicable to all sky conditions. The presence of atmospheric disturbance factors, such as thin clouds and precondensation aerosol clouds, may have affected the PWV.

The performance of the estimated PWV data from Eq. (7) was validated against the mean daily values for nighttime (0000 UT) and daytime (1200 UT) and against the mean monthly and yearly values for the whole dataset (1985–2012). The results of these comparisons are presented in

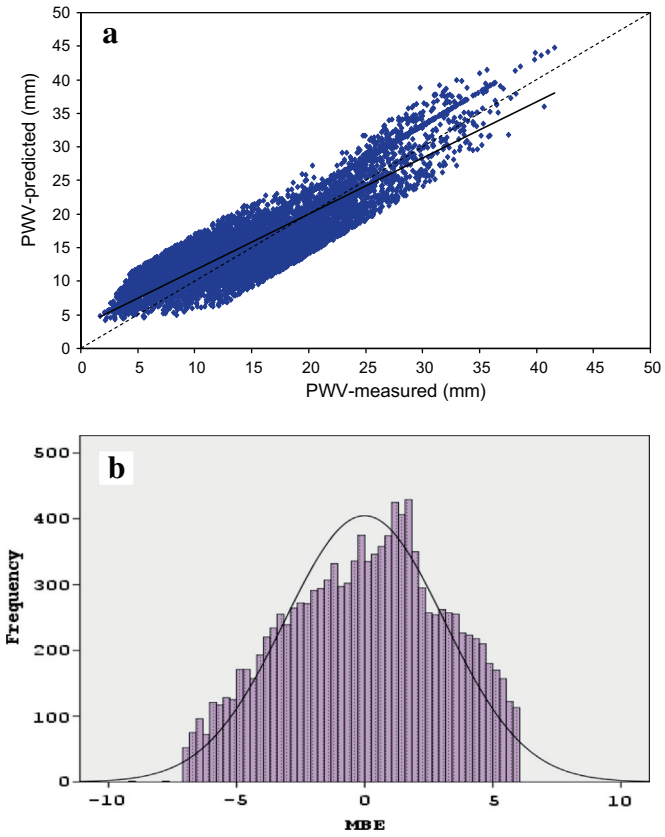

Figure 2 (a) Comparisons between the measured PWV and the predicted PWV using Eq. (7) for the dataset spanning the period 1985–2007. The dashed line is the regression fit between the measured and predicted PWV values. The solid line is a 1:1 line for reference. (b) A histogram showing the frequency distribution of the MBE (mm) of the measured–predicted PWV values superimposed on a normal distribution curve.

columns 2–6 of Table 2.The statistical parameters for all the selections do not greatly differ from the originally proposed parameters. With the exception of the nighttime monthly mean data, which showed an MBE value of 1.82 mm, the rest of the data had MBE values less than 1 mm.

3.2. Model validation: independent datasets

The performance of Eq. (7) was validated with two independent datasets, set 1 and set 2. The statistics describing the agreement between the model predictability and the measured data from both sets are given in the last two columns of Table 2. The RMSE values for set 1 and set 2 were 3.21 mm and 2.63 mm, respectively. The MBE and MPE values were below 1 mm and within ± 10%, respectively. The mean predicted PWV values for set 1 and set 2 were 15.23 and 11.63 mm, respectively. This finding is comparable with the mean measured values for set 1 (15.12 mm) and for set 2 (12.74 mm). Fig. 3a shows the predicted PWV plotted against the measured PWV for set 1. Most of the data are close to the 1:1 line, with a maximum deviation from that line of no more than 7 mm. The distribution of the MBE is presented in Fig. 3b, which resembles a normal distribution.

Fig. 4a shows the predicted PWV versus the measured values for set 2. Although the data are distributed around the 1:1 line at medium values (7–14 mm), the data are farther from that line for PWV values below 7 mm and higher than 14 mm. The maximum deviation of the PWV values occurs in these two intervals, however, does not exceed 6 mm. Fig. 4b shows the distribution of the MBE for set 2, which resembles a normal distribution.

Many factors may cause these deviations, e.g., the uncertainties in predicting the PWV using Eq. (7) are greater in some extreme atmospheric conditions, such as a heat wave on hot summer days and temperature inversions in the lower atmospheric levels during the cold winter nights. Clouds may also affect the predictive ability of the model. The instrumental uncertainties associated with the sun photometer-derived PWV values may introduce some additional error in the measurements. The PWV deduced from the sun photometer is concentrated at one wavelength band (940 mm), whereas water vapour has strong emission lines at other wavelengths. Despite these possibilities, Eq. (7) still predicts the PWV with reasonable accuracy from the obtained statistical parameters.

3.3. Selected model assessments

Numerous studies have demonstrated the existence of correlations between the PWV and surface humidity parameters, such as water vapour pressure, dew-point temperature, and absolute and relative humidity. As a result, different formulae have been proposed. Reviews of such parameterisations are usually presented in connection with studies on the attenuation of solar radiation components, e.g., Iqbal (1983).

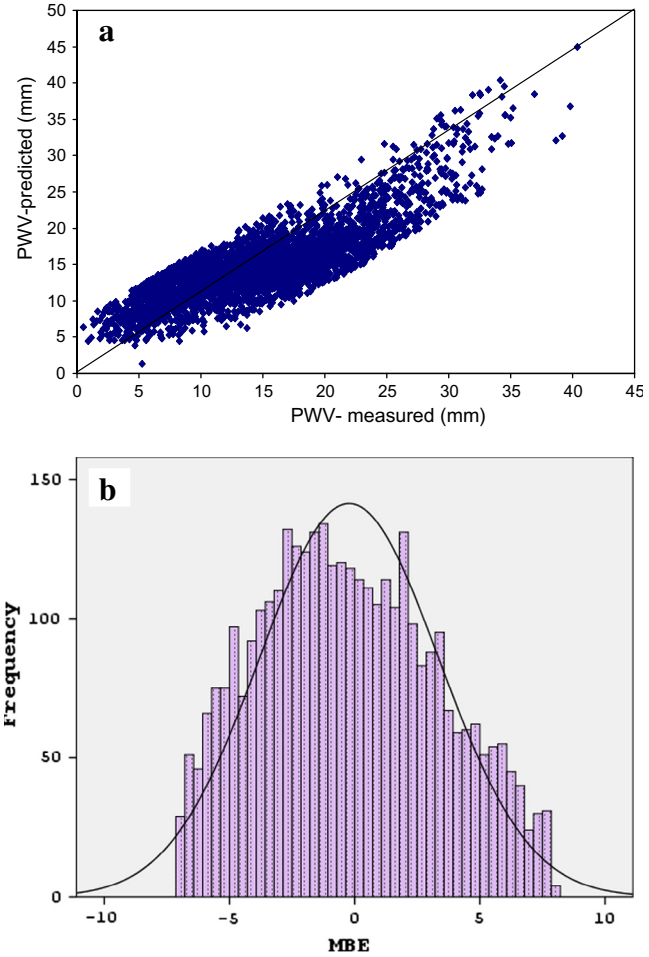

Figure 3 (a) Shows the measured PWV versus the predicted PWV obtained using Eq. (7) for the dataset covering the period 2008–2012. The dashed line is the regression fit between PWV Predicted and PWV Measured. The solid line is the 1:1 line. (b) A histogram showing the frequency distribution of the MBE (mm) of the measured–predicted PWV values superimposed on a normal distribution curve.

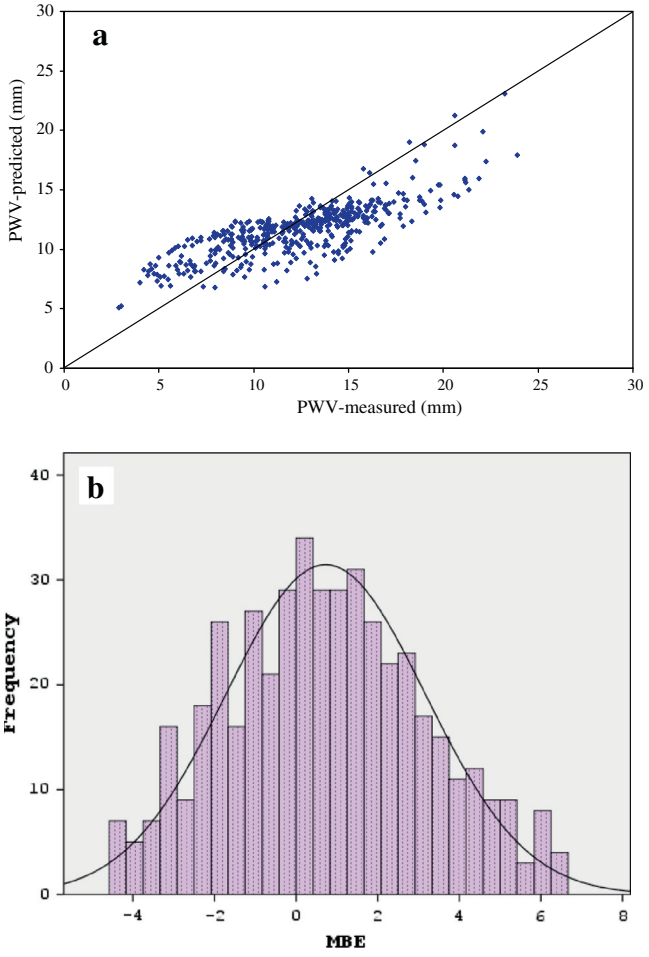

Figure 4 (a) The sun photometer-derived PWV data at 940 nm for the period 2001–2002 plotted against the predicted PWV using Eq. (7). The dashed line is the regression fit between PWV Predicted and PWV Measured. The solid line is the 1:1 line for reference. (b) A histogram showing the frequency distribution of the MBE (mm) of the measured–predicted PWV values superimposed on a normal distribution curve.

The objective of this section is to assess the performance of some of the previously reported PWV models for Riyadh and to compare their performance with the model obtained in this study (Eq. (7)). Fifteen models were selected that differ from each other in terms of the number of variables and the model (linear, exponential or quadratic). The predictability of these models was tested against the dataset that covers the period 1985–2007 which were used to constrain the proposed model (Eq. (7)).

The functional form, the mean PWV values, and the statistics (RMSE and MBE) describing the agreement between the tested models and the observed PWV are given in Table 3. The RMSE values for the models ranged between 3.54 and 10.78 mm. The MBE ranged between −3.36 and 9.67 mm. According to their MBE and RMSE values, the models of Hussain (1984) and Butler (1998a,b) had the worst predictabilities against the measured values. On the other hand, Adeyemi (2009) model for Kano showed the best performances according to its MBE and RMSE. Gate model (cited by Kambezidis et al., 1993) showed next best model. The other models had reasonable MBE values. Four of these models showed MBE values less than ±3 mm, and four models presented values between 3 and 4 mm. Nearly all of the models overestimated the measured PWV values to different extents. The Evnevich (1967) model and Adeyemi (2009) model for Lagos underestimated the measured values.

The multilinear model proposed in this study outperformed the overall performance of the other models.

The unsuccessful prediction of PWV in Riyadh by these models does not mean that they are entirely inaccurate. The models were proposed for sites with different atmospheric conditions than those in Riyadh. Thus, these models may over- or underestimate measurements at other sites. For instance, Adeyemi (2009) model to estimate the PWV for Lagos overestimates the predictability of PWV in Riyadh, because Lagos is a very humid place. Contrary the predictability of Adeyemi (2009) model for Kano (semiarid place) matches the measured PWV because it has similar atmospheric conditions found in Riyadh.

In certain applications, such as modelling the attenuation of direct solar radiation, an appropriate model to quantify the atmospheric water content may need to be selected. In Saudi

Table 3 The functional forms of 15 selected models. The statistical parameters for the considered models (mean PWV values, MBE, and RMSE) are compared with the measured values for Riyadh using daily data (mean PWV = 15.24) for the period 1985–2007. The RMSE, MBE for Eq. (7) were in respective −0.06 and 2.80 mm. All the parameters are in mm.

Model	Functional form	PWV	MBE	RMSE
Hann (cited by Okulov et al., 2007)	$PWV = 2.1 \times eo$	14.73	0.51	6.12
Gate (cited by Kambezidis et al., 1993)	$PWV = 2.3 \times eo \times 10^{-H(station)/22{,}000}$	14.90	0.34	5.43
Sivkov (1971)	$PWV = 3.8 \times eo^{2/3}$	13.64	1.60	4.73
Evnevich (1967)	$PWV = 1.6 \times eo + 2.3$	17.52	−2.28	7.01
Reitan (1963)	$\ln(PWV) = 0.1102 + 0.06138 \times t_d$	10.32	4.92	6.82
Leckner (1978)	$PWV = 493 \times eo \times T^{-1}$	11.83	3.41	6.34
Won (1977), cited by Iqbal (1983)	$PWV = 0.11 \times \exp[(2.2572 + 0.05454 \times t_d)]$	10.47	4.77	7.15
Okulov et al. (2007)	$PWV = 1.58 \times eo + 0.68$	12.01	3.23	5.34
Ruckstuhl et al. (2007)	$PWV = 2.67 \times q^{0.6}$	13.43	1.81	5.67
Hussain (1984)	$PWV = RH \times (4.7923 + 0.364 \times T + 0.0055 \times T^2 + 0.0003 \times T^3)$	5.48	9.76	10.78
Butler (1998a)	$PWV = \frac{m_w P_0 H}{\rho k T_0}$	8.61	6.63	8.61
Adedokun (1986)	$PWV = 0.0273 q^{1.551}$	11.35	3.89	7.15
Adeyemi (2009) (Lagos)	$PWV = 226 \times r_s - 0.050$	18.61	−3.36	6.41
Adeyemi (2009) (Kano)	$PWV = 480 \times r_s - 0.216$	14.93	0.31	3.54

Footnote: eo is the screen-level vapour pressure, T is the screen-level temperature, t_d is the dew point temperature, and PWV is the precipitable water vapour. q is the specific humidity; r_s is the mixing ratio at screen level. In Butler (1998) model P_0 is the water vapour partial pressure at the surface in μbar, H is the scale height of water vapour (assumed to be 1.5 km), m_w is the molecular weight of water, k is the Boltzmann constant, and T_0 is the surface temperature in K.

Arabia and other locations with similar atmospheric conditions, the proposed model could accurately predict the PWV.

4. Conclusion

We have developed a simple relationship to predict the PWV using the screen-level temperature and vapour pressure. The multilinear model can predict the integrated water content with reasonable accuracy in the central region of Saudi Arabia and at any location with similar atmospheric conditions. The model showed excellent prediction ability when tested against four and half years of independent data obtained by radiosonde. The model performed well against two years of independent PWV measurements obtained with a sun photometer at 940 nm. The predictions by the proposed model were excellent when compared with 15 previously reported models.

Acknowledgments

The authors thank the Saudi Presidency of Meteorological and Environment (PME) for kindly providing the radiosonde and surface climate data. The authors also would like to thank the King Abdulaziz City for Science and Technology (KACST) for supporting this work. We also would like to thank the reviewers for their valuable comments and suggestions.

References

Adeyemi, B., 2009a. Empirical modeling of layered integrated water vapor using surface mixing ratio in Nigeria. J. Appl. Meteor. Climatol. 48 (2), 369–380.

Adeyemi, B., 2009b. Empirical formulations for inter-layer precipitable water vapor in Nigeria. Pacific J. Sci. Technol. 10 (2), 35–45.

Adedokun, J.A., 1986. On a relationship for estimating precipitable water vapour aloft from surface humidity over West-Africa. J. Climatol. 6, 161–172.

Bevis, M., Businger, S., Herring, T.A., Rocken, C., Anthes, R.A., Ware, R.H., 1992. GPS meteorology. Remote sensing of atmospheric water vapour using the Global Positioning System. J. Geophys. Res. 97, 15784–15801.

Bokoye, A.I., Royer, A., O'Neill, N.T., Cliche, P., McArthur, L.J.B., Teillet, P.M., Fedosejevs, G., Thériault, J.M., 2003. Multisensor analysis of integrated atmospheric water vapor over Canada and Alaska. J. Geophys. Res. 108, 4480. http://dx.doi.org/10.1029/2002JD002721.

Brooks, D.R., Mims, F.M., Roettger, R., 2007. Inexpensive near-IR sun photometer for measuring total column water vapor. J. Atmos. Oceanic Technol. 24, 1268–1276.

Butler, B., 1998a. Precipitable Water at VLA 1990–1998. MMA Memo. No. 237.

Butler, B., 1998b. Precipitable Water at KP 1993–1998. MMA Memo. No. 238.

Clay, R.W., Wild, N.R., Bird, D.J., Dawson, B.R., Johnston, M., Patrick, R., Sewell, A., 1998. A cloud monitoring system for remote sites. Publ. Astronom. Soc. Australia 15, 332–335.

Cohen, J.L., Salstein, D.A., Rosen, R.D., 2000. Interannual variability in the meridional transport of water vapor. J. Hydrometeor. 1, 547–553.

Dai, A., Wang, J., Ware, R.H., Hove, T.V., 2002. Diurnal variation in water vapor over North America and its implications for sampling errors in radiosonde humidity. J. Geophys. Res. 107, 4090. http://dx.doi.org/10.1029/2001JD000642.

Dupont, J.C., Haeffelin, M., Drobinski, P., Besnard, T., 2008. Parametric model to estimate clear-sky long wave irradiance at the surface on the basis of vertical distribution of humidity and temperature. J. Geophys. Res. 113, D07203. http://dx.doi.org/10.1029/2007JD009046.

Elies, C., Bech, J., Rodríguez-Marcos, J., Sola, Y., Lorente, J., 2010. A comparison of total precipitable water measurements from radiosonde and sun photometers. Atmos. Res. 97, 385–392.

Elliott, W.P., Gaffen, D.J., 1991. On the utility of radiosonde humidity archives for climate studies. Bull. Am. Meteor. Soc. 72, 1507–1519.

Eng, R.S., Kelley, P.L., Mooradian, A., Calawa, A.R., Harman, T.C., 1973. Tunable laser measurements of water vapor transitions in the vicinity of 5 μm. Chem. Phys. Lett. 19 (15), 524–528.

Evnevich, T.V., 1967. Computation of direct solar radiation and the transparency coefficient. Meteorology and Hydrol. 5, 106–109.

Free, M., Angell, J.K., Durre, I., Lanzante, J., Peterson, T.C., Seidel, D.J., 2004. Using first differences to reduce inhomogeneity in radiosonde temperature datasets. J. Climate 17, 4171–4179.

Follette, M.B., Hudson, R.D., Nedoluha, G.E., 2008. Classification of Northern Hemisphere stratospheric ozone and water vapor profiles by meteorological regime. Atmos. Chem. Phys. Discuss. 8 (4), 13375.

Gerding, M., Christoph, R., Marion, M., Roland, N., 2004. Tropospheric water vapour soundings by lidar at high Arctic latitudes. Atmos. Res. 71 (4), 289–302.

Guerova, G., Brockmann, E., Schubiger, F., Morland, J., Mätzler, C., 2005. An integrated assessment of measured and modeled integrated water vapor in Switzerland for the period 2001–03. J. Appl. Meteorol. 44 (7), 1033–1044.

Gueymard, C., 1994. Analysis of monthly average atmospheric precipitable water and turbidity in Canada and northern United-States. Solar Energy 53, 57–71.

Hagemann, S., Bengtsson, L., Gendt, G., 2003. On the determination of atmospheric water vapor from GPS measurements. J. Geophys. Res., 4678.

Holben, B.N., Tanre, D., Smirnov, A., Eck, T.F., Slutsker, I., et al., 2001. An emerging ground-based aerosol climatology: aerosol optical depth from AERONET. J. Geophys. Res. 106, 12067–12097.

Hsu, S.A., Blanchard, B.W., 1989. The relationship between total precipitable water and surface level humidity over the sea surface—A further evaluation. J. Geophys. Res 94, 14 539–14 545.

Hussain, M., 1984. Estimation of global and diffuse irradiation from sunshine duration and atmospheric water vapour content. Solar Energy 33 (2), 217–220.

Iqbal, M., 1983. An Introduction to Solar Radiation. Academic Press, New York.

Kassomenos, P.A., MCGregor, G.R., 2006. The interannual variability and trend of precipitable water over Southern Greece. J. Hydrometerol. 7, 1–14.

Kambezidis, H.D., Founda, D.H., Papanikolau, N.S., 1993. Linke and Unsworth-Monteith turbidity parameters in Athens. Quart. J. Roy. Meteorol. Soc. 119, 367–374.

Kuwahara, T., Mizuno, A., Nagahama, T., Maezawa, H., Morihira, A., Toriyama, N., Murayama, S., Matsuura, M., Sugimoto, T., Asayama, S., Mizuno, N., Onishi, T., Fukui, Y., 2008. Ground-based millimeter-wave observations of water vapor emission (183 GHz) at Atacama, Chile. Adv. Space Res. 42 (7), 1167–1171.

Lanzante, J.R., Klein, S.A., Seidel, D.J., 2003. Temporal homogenization of monthly radiosonde temperature data. Part II: Methodology. J. Climate 16, 224–240.

Leckner, B., 1978. The spectral distribution of solar radiation at the earth surface elements of a model. Solar energy 20 (2), 143–150.

Lhomme, J.P., Vacher, J.J., Rocheteau, A., 2007. Estimating downward long-wave radiation on the Andean Altiplano. Agric. For. Meteorol. 145, 139–148.

Li, G., Kimura, F., Sato, T., Huang, D., 2008. A composite analysis of diurnal cycle of GPS precipitable water vapor in central Japan during Calm Summer Days. Theoret. Appl. Climatol. 92 (1/2), 15.

Maghrabi, A.H., Clay, R.W., Dawson, B., Wild, N., 2009. Design and development of a simple infrared monitor for cloud detection. Energy Conserv. Manage. http://dx.doi.org/10.1016/j.enconman.2009.06.029.

Maghrabi, A.H., 2009. Parameterization of a simple model to estimate monthly global solar radiation based on meteorological variables, and evaluation of existing solar radiation models for Tabouk, Saudi Arabia. Energy Conserv. Manage. 50, 2754–2760.

Maghrabi, A.H., Clay, R.W., 2010. Precipitable water vapour estimation on the basis of sky temperatures measured by a single-pixel IR detector and screen temperatures under clear skies. J. Meteorol. Appl. 17, 279–286.

Maghrabi, A., Alharbi, B., Tapper, N., 2011. Impact of the March 2009 dust event in Saudi Arabia on aerosol optical properties, meteorological parameters, sky temperature and emissivity. Atmos. Environ. 13 (45), 2164–2173.

Okulov, O., Ohvril, H., Kivi, R., 2007. Atmospheric precipitable water in Estonia, 1990–2001. Bor. Environ. Res. 7, 291–300.

Pramualsakdikul, S., Haas, R., Elgered, G., Scherneck, H.G., 2007. Sensing of diurnal and semi-diurnal variability in the water vapour content in the tropics using GPS measurements. Meteorol. Appl. 14, 403–412.

Reitan, C.H., 1963. Surface dew point and water vapor aloft. J. Appl. Meteorol. 2, 776–779.

Ruckstuhl, C., Philipona, R., Morland, J., Ohmura, A., 2007. Observed relationship between surface specific humidity, integrated water vapor, and longwave downward radiation at different altitudes. J. Geophys. Res. 112, D03302. http://dx.doi.org/10.1029/2006JD007850.

Sivkov, S.I., 1971. Computation of solar radiation characteristics. Israel Program for Scientific Translations, Jerusalem, 185 pp (translated from Russian).

Smirnov, V.V., Moore, G.W.K., 2001. Short-term and seasonal variability of the atmospheric water vapor transport through the Mackenzie River basin. J. Hydrometeor. 2, 441–452.

Stoew, B., Elgered, G., Johansson, J.M., 2001. An assessment of estimates of integrated water vapor from ground-based GPS data. Meteorol. Atmos. Phys. 77, 99–107.

Torres, B., Cachorro V.E., Toledano, C., Ortiz de Galisteo, J.P., Berjón, A., de Frutos, A.M., Bennouna, Y., Laulainen, N., 2010. Precipitable water vapor characterization in the Gulf of Cadiz region (southwestern Spain) based on Sun photometer, GPS, and radiosonde data. J. Geophys. Res. 115, D18103, 11 pp. doi:10.1029/2009JD012724.

Tuller, S., 1977. The relationship between precipitable water vapour and surface humidity in New Zealand. Arch. Meteor. Geophys. Bioklim. A26, 197–212.

Viswanadham, Y., 1980. The relationship between total precipitable water and surface dew point. J. Appl. Meteorol. 20 (1), 3–6.

Wang, J., Cole, H.L., Miller, E.R., Beierle, K., Paukkunen, A., Laine, T.K., 2002. Correction of humidity measurement errors from Vaisala RS80 radiosonde Application to TOGA COARE data. J. Atmos. Oceanic Technol. 19, 981–1002.

Zhai, P., Eskridge, R.E., 1996. Analyses of inhomogeneities in radiosonde temperature and humidity time series. J. Climate 9, 884–894.

Zhai, P., Eskridge, R.E., 1997. Atmospheric water vapor over China. J. Climate 10, 2643–2652.